



***In silico* analysis of Potential Phytochemical Constituents of *Orthosiphon stamineus* as
Significant Inhibitors Against Urolithiasis**

Bharathi N* & Caroline Nirmala R

Department of Plant Molecular Biology and Bioinformatics, Centre for Plant Molecular Biology and
Biotechnology, Tamil Nadu Agricultural University, Coimbatore, India

Author's email ID: bharathi.n@tnau.ac.in

Received: 21stSeptember, 2023

Revised: 22nd, October, 2023

Revised: 25th, October, 2023

Accepted: 20th, December, 2023

ABSTRACT

Naturally occurring bioactives from plant sources have played a significant role in developing multi-targeted drugs towards treatment of various human ailments. Urolithiasis is the process of stone formation in the kidney, urinary tract or in bladder. It occurs to 1 in 20 people at different phases of their life causing pain in the abdomen, flank or groin and bloody urine at times. The current study focuses on phytochemical activity of *Orthosiphon stamineus* (Java tea) that can act against kidney stone. The target proteins responsible for stone formation were identified through literature search and the three dimensional structures available were retrieved from Protein Data Bank and structures unavailable were modelled through computational methods. These proteins were docked against the phytochemicals and certain synthetic compounds which are commercially used for Urolithiasis. The best docked compounds and their interaction have been studied and it was identified that when compared to the synthetic compounds, there is high

competence for phytochemicals in binding to the target proteins which suggests that these compounds can be used further for the process of designing a drug effectively against urolithiasis.

Keywords: Urolithiasis, *Orthosiphon stamineus*, Java tea, Phytochemical and Synthetic compounds

INTRODUCTION

Urolithiasis being the most common disease occurring in the urinary tract is known to affect about 12% of the world population. Less water intake and imbalanced nutrient diet are the major risk factors paving way to urolithiasis (López, M & Hoppe, B, 2010). The symptoms of kidney stone disorder depends on the location where it is formed, whether it is in the kidney, ureter or urinary bladder. Though the initial stage shows no sign of occurrence, the lateral stage causes intensive cramping pain, hematuria, urinary tract related disorders and in severe cases all ending up with kidney dilation (hydronephrosis). The kidney stone formation possess high risk of association with other chronic diseases viz., diabetes, hypertension and renal failure. kidney stone disorder can be cured effectively if the mechanisms involved in stone formation is understood clearly. (Alelign, T, & Petros, B. 2018).

The surgical methods that are used to remove the kidney stones being painful, it is always wiser to prefer the preventive measures that cause no pain. Nowadays the usage of products derived from plants, animals and marine resources are high in use. In traditional Indian medicine, plants play a vital role as the curative agents. **Herbal plants** are an important source of medicines and major health care providers across the globe since ancient times. (Kumar, M, Patel, M et al., 2021). One such plant is *Orthosiphon stamineus* of the family *lamiaceae*. This plant is known for its diverse bioactive characteristic such as antihypertensive, antioxidant, anti-inflammatory, hepatoprotective and hypoglycaemic. It is reported that *Orthosiphon stamineus* having many compounds that can act as the best inhibitors against the proteins responsible for Urolithiasis. (Hsu, C. L et al., 2010)

MATERIAL AND METHODS

Selection of targets

S.No	Pdb id	Swiss-prot id	Protein targets	Role of target proteins in Urolithiasis
1.	1KB2	P11473	Vitamin D3 Receptor(Chains A,B)	Increases digestive Calcium absorption and promotes urinary stone formation (Letavernier, E., & Daudon, M. (2018).)
2.	1UUH	P16070	CD44 ANTIGEN(Chains A,B)	A cell surface receptor, play a notable role in Calcium Oxalate binding (Asselman, M <i>et al.</i> , 2003)
3	-	Q8N6F1	Claudin 19 (Modelled protein)	Renal calcium and magnesium wasting(Hypercalciuria&hypomagnesemia)
4.	5FUO	P02768	SERUM ALBUMIN(Chain A)	Promotes the growth of Calcium Oxalate Monohydrate crystals on hydroxyapatite with Citrate & magnesium inhibitors (Ebrahimpour, A <i>et al.</i> , 1991)

5.	1BT6	P60903	Annexin II	Binds Calcium Oxalate Monohydrate crystals on renal tubular cells (Kumar <i>et al.</i> , 2003)
6.	1POZ	P16070	Hyaluronan synthase	Retention of Calcium Oxalate crystals in tubular epithelial cells (Asselman, Met <i>et al.</i> , 2003)
7.	1IQT	Q14103	Heterogeneous nuclear ribonucleoprotein DO	It's acidic peptide sequence will mediate the attachment of Calcium Oxalate crystals to the renal tubular cells through selective absorption. (Sorokina, <i>et al.</i> , 2004)

Target protein structure retrieval:

Three dimensional X-ray crystal structures for the target proteins were obtained from the Protein Data Bank. The PDB ID of corresponding proteins was tabulated above. The protein Claudin 19 does not have experimentally determined 3D structure and hence it was computationally modeled through Swiss model.

Active site prediction

The Computed Atlas of Surface Topography of proteins (CASTp) 3.0 (Binkowski TA, *et al.*, 2003&Tian *et al.*, 2018)) was used to predict the active sites that were present in the protein structure. This online server was used in identification and measurement of voids on 3D protein structures. The 3D protein structure was submitted to the CASTp server and binding site residues was predicted.

Selection of ligands

Compounds from *Orthosiphon stamineus* was identified through various literature sources and of about 136 phytochemicals have been retrieved from PubChem and was used for virtual screening against the potential targets for Urolithiasis. (Table 1)

ADME property calculation

ADMET properties help to have insight into the pharmacokinetic nature of the ligand compounds. The phytochemical compounds saved in Canonical SMILES format was uploaded to Swiss ADME available in SIB (Swiss Institute of Bioinformatics) webserver (<https://www.sib.swiss>) and submitted for ADME estimation. The details of aqueous solubility, blood brain barrier level, gastrointestinal absorption, CYP 2D6, Hepatotoxicity, plasma protein binding levels and the drug- likeliness parameters were noted and analyzed. The library was taken for Docking studies along with seven targets using PyRx.

Virtual Screening

Virtual screening was performed using Python Prescription Virtual Screening tool (PyRx 0.8) containing AutoDock Vina module (Dallakyan and Olson, 2015). Protein structure was prepared by adding hydrogen atoms and energy minimization was done. The docking analysis was performed for the chosen compounds with the target proteins using AutoDock Vina module in PyRx 0.8. For docking, the grid map was fixed on the ligand binding site of the receptor. Binding sites were predicted using CASTP server and the same were used for setting grid (XYZ dimensions: 25*25*25) in the Auto Dock Vina for virtual screening experiment with the exhaustiveness value of 8.

RESULTS AND DISCUSSION

Virtual screening of potential herbal ligands against major protein targets for Urolithiasis

Virtual screening of 136 ligands from Java tea 7 major protein targets of Urolithiasis identified potential inhibitors. Information regarding the binding site residues predicted using CASTp server. Top 10 hits reported with higher binding affinity for each target protein is considered for further interaction analysis.

Annexin II

For the target 1BT6 phytochemical compounds such as Beta amyron, Orthosiphol X, masilinic acid, Catechin gallate have better binding affinity with binding scores of -7.8, -7.7, -7.7, -7.5 Kcal/mol respectively with hydrogen bond formation. (Fig 1)

Heterogeneous nuclear ribonucleoprotein

For the target protein 1IQ7 phytochemical compounds such as (-)-Catechin gallate, Beta amyron, Orthosiphol X, Rutin, Sitosterol, cianidanol and Quercetin were predicted as best compounds with

binding affinity values -7.5, -7.4, -7.3, -7.1, -7.1, -7.2 and -7.3 Kcal/mol respectively by forming stable hydrogen bonds.(Fig 1)

Vitamin D3 Receptor

Vitamin D3 receptor chains A and B acts as a main target for urolithiasis and the 3D structure of 1KB2 target was retrieved from PDB. Compounds such as catechin gallate, Quercetin, Orthosiphon_A, neoorthosiphonol with least binding affinity were predicted such as -8.1, -7.5, -7.4 and -7.2Kcal/mol respectively. (Fig 1)

Hyaluronan synthase

For the given target 1POZ phytochemical compounds such as Orthosiphon A, Rutin, Orthosiphon B, Masilinic acid, hyperin, eupatorin were found to interact with good binding scores of -6.6,-6.8,-6.4,-6.5,-6.9 and -6.8 Kcal/mol respectively.(Fig 1)

CD44 ANTIGEN

The crystal structure of CD 44 Antigen was retrieved from PDB and phytochemical compounds such as Orthosiphon X, Rutin, Oleanolic acid, Beta amyron, hyperin, rosmarinic acid, betulinic acid and Orthosiphon M were found to interact well with the target protein with binding scores of -8.5,-7.9,-7.8,-7.7,-7.7, -7.8,-7.9 and -7.6Kcal/mol respectively.(Fig 1)

SERUM ALBUMIN

For the target 5FUO phytochemical compounds such as (-)-Catechin gallate, betulinic acid, Orthosiphon A, neoorthosiphonol A interacted well with binding scores of -10.5,-10.4,-10.1 and - 8.9 Kcal/mol respectively.(Fig 1)

Claudin 19

The structure of the protein Claudin 19 was modeled using swissmodel. The phytochemicals such as Orthosiphon A, Betulinic acid, Stigmasterol, , Orthosiphon N and staminol A shows interaction with binding affinity of -9.8,-9.3,-9.2, -9.1 and -8.9 Kcal/mol respectively.(Fig 1)

CONCLUSION

As a result, phytochemical compounds of *Orthosiphon stamineus* have better binding affinity towards the targets like 1BT6, 1IQT, 1KB2, 1POZ, 1UUH, 5FUO, and Claudin 19. In most of the target proteins the compounds such as Orthosiphon X, Rutin, (-)-Catechin gallate and Masilinic acid were found to interact with good binding affinity and forming more number of hydrogen bonds. While considering

the side effects of the synthetic drugs, it was obvious that there is still a greater demand for the safer and effective therapy for treating Urolithiasis. In the current study, the ADME profiling of the phytochemical compounds from *Orthosiphon stamineus* ensured its drug- likeliness behavior besides its interaction with the target proteins of Urolithiasis. The results suggested the possibility of employing these compounds as the alternative source of Urolithiasis. Thus, the present preliminary study may direct the research attention on the phytochemical compounds for treating Urolithiasis.

Table1: List of compounds identified from *Orthosiphon stamineus*

S.No	Compound ID	Compound name	Molecular formula	Molecular weight(g/mol)
1.	240	Benzaldehyde	C₇H₆O	106.12
2.	370	Galic acid	C₇H₆O₅	170.12
3.	892	Inositol	C₆H₁₂O₆	180.16
4.	931	Naphthalene	C₁₀H₈	128.169
5.	998	Phenylacetaldehyde	C₈H₈O	120.15
6.	1175	Uric acid	C₅H₄N₄O₃	168.11

7.	2153	Theophylline(xanthine)	<u>C₇H₈N₄O₂</u>	180.16
8.	2519	Caffeine	<u>C₈H₁₀N₄O₂</u>	194.19
9.	2537	Camphor	<u>C₁₀H₁₆O</u>	152.23
10.	2758	Cineole	<u>C₁₀H₁₈O</u>	154.25
11.	3314	Eugenol(caryophyllic acid)	<u>C₁₀H₁₂O₂</u>	164.2
12.	5429	Dimethylxanthine	<u>C₇H₈N₄O₂</u>	180.16
13.	6184	Hexanal	<u>C₆H₁₂O</u>	100.16
14.	6448	Isobornyl acetate	<u>C₁₂H₂₀O₂</u>	196.29
15.	6616	Cophene	<u>C₁₀H₁₆</u>	136.23
16.	6654	Alpha pinene	<u>C₁₀H₁₆</u>	136.23
17.	6949	Beta guaiene	<u>C₁₅H₂₄</u>	204.35
18.	6986	Isomethone	<u>C₁₀H₁₈O</u>	154.25
19.	7055	2- methylnaphthalene	<u>C₁₁H₁₀</u>	142.2
20.	7127	Methyleugenol	<u>C₁₁H₁₄O₂</u>	178.23
21.	7439	Carvone	<u>C₁₀H₁₄O</u>	150.22
22.	7463	Para -cymene	<u>C₁₀H₁₄</u>	134.22
23.	8175	Decanal	<u>C₁₀H₂₀O</u>	156.26
24.	8182	Dodecane	<u>C₁₂H₂₆</u>	170.33
25.	8842	Citronellol	<u>C₁₀H₂₀O</u>	156.26
26.	8815	Estragole	<u>C₁₀H₁₂O</u>	148.2
27.	9064	Cianidanol	<u>C₁₅H₁₄O₆</u>	290.27
28.	9895	Beta-cyclocitral	<u>C₁₀H₁₆O</u>	152.23
29.	10123	Alpha-selinene	<u>C₁₅H₂₄</u>	204.35

30.	10494	Oleanolic acid	C₃₀H₄₈O₃	456.7
31.	11527	Octanal-3-ol	C₈H₁₈O	130.229
32.	12388	Tridecane	C₁₃H₂₈	184.36
33.	14257	Hendecane	C₁₁H₂₄	156.31
34.	14896	Beta-pinene	C₁₀H₁₆	136.23
35.	14985	5,7,8-trimethyltol	C₂₉H₅₀O₂	430.7
36.	19602	2-pentylfuran	C₉H₁₄O	138.21
37.	19725	Alpha-copaene	C₁₅H₂₄	204.35
38.	22311	Limonene	C₁₀H₁₆	136.23
39.	26447	Menthone	C₁₀H₁₈O	154.25
40.	61041	Safranal	C₁₀H₁₄O	150.22
41.	62127	Caryophyll acetate	C₁₇H₂₈O₂	264.4
42.	64685	Borneol	C₁₀H₁₈O	154.25
43.	64971	Betulinic acid	C₃₀H₄₈O₃	456.7
44.	68316	Perillene	C₁₀H₁₄O	150.22
45.	73170	Alpha amyrin	C₃₀H₅₀O	426.7
46.	73659	Masilinic acid	C₃₀H₄₈O₄	472.7
47.	75324	Tetrametyluric acid	C₉H₁₂N₄O₃	224.22
48.	79730	4,5,7-trimethoxyflavone	C₁₈H₁₆O₅	312.3
49.	81722	Alpha,alpha,-dimethyl-4-methyl enecyclohexanemethanol	C₁₀H₁₈O	154.25
50.	86609	Alpha cubenene	C₁₅H₂₄	204.35
51.	87529	Beta cubenene	C₁₅H₂₄	204.35

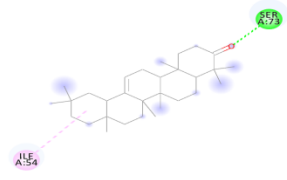
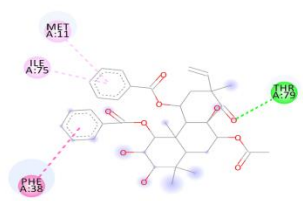
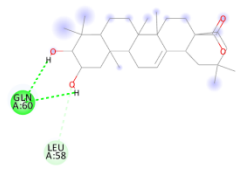
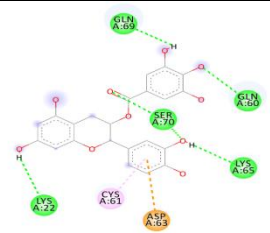
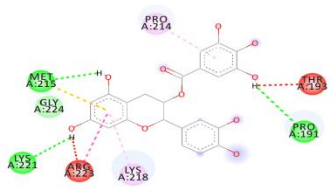
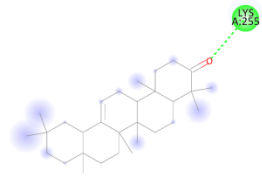
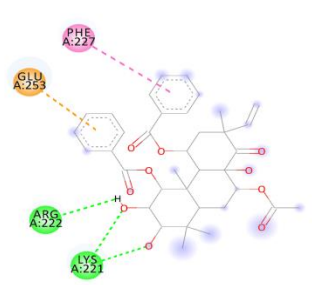
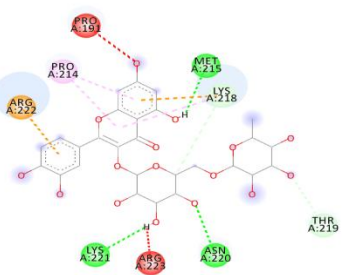
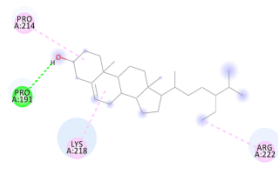
52.	96118	Tetramethyl-o-scutellarin	C₁₉H₁₈O₆	342.3
53.	97214	Eupatorin	C₁₈H₁₆O₇	344.3
54.	145659	Sinensetin	C₂₀H₂₀O₇	372.4
55.	157983	2-pent-1-enylfuran	C₉H₁₂O	136.19
56.	161271	Salvigenin	C₁₈H₁₆O₆	328.3
57.	177148	1-(7,8-dimethoxy-2,2-dimethyl-chromen-6-yl)ethanone	C₁₅H₁₈O₄	262.3
58.	188323	Crisimaritin	C₁₇H₁₄O₆	314.29
59.	222284	Beta- sitosterol	C₂₉H₅₀O	414.7
60.	292285	Octadecane	C₂₆H₅₄	366.7
61.	324224	Beta-bourbonene	C₁₅H₂₄	204.35
62.	439378	L-theanine	C₇H₁₄N₂O₃	174.2
63.	441005	(+)-delta-cadinene	C₁₅H₂₄	204.35
64.	445858	Ferulic acid	C₁₀H₁₀O₄	194.18
65.	519382	Dihydro-beta-inone	C₁₃H₂₂O	194.31
66.	543423	1,2-15,16-diepoxyhexadecane	C₁₆H₃₀O₂	254.41
67.	584957	1,3,3-trimethyl-2-vinyl-1-cyclohexane	C₁₁H₁₈	150.26
68.	608753	Beta-vatrienene	C₁₅H₂₂	202.33
69.	631170	Luteolin tetramethyl ether	C₁₉H₁₈O₆	342.3
70.	637182	Orthosiphol v	C₃₃H₄₂O₁₁	614.7
71.	637563	Anethole	C₁₀H₁₂O	148.2
72.	638014	Beta-ionone	C₁₃H₂₀O	192.3
73.	638072	Squalene	C₃₀H₅₀	410.7

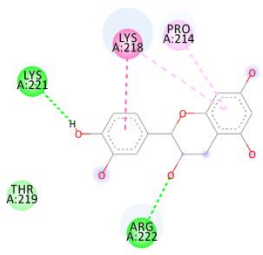
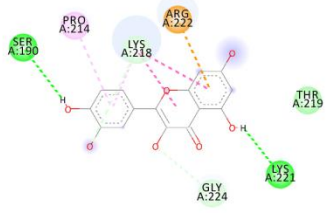
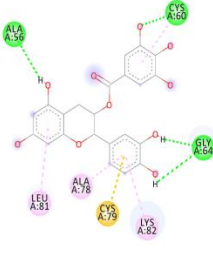
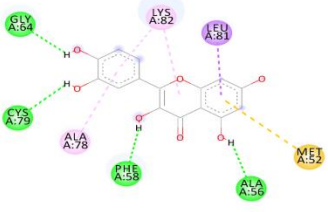
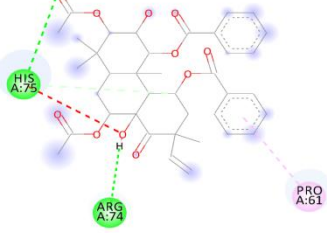
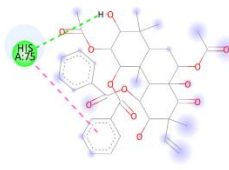
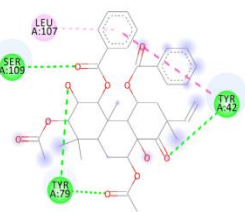
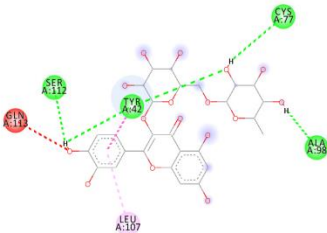
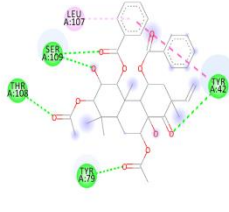
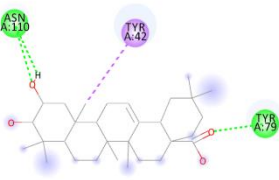
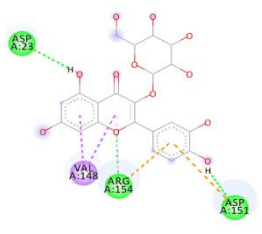
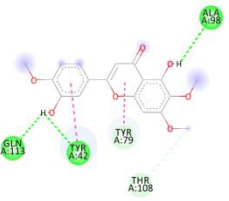
74.	689043	Caffeic acid	C₉H₈O₄	180.16
75.	1163236	2-(3,4-dimethoxyphenyl)-5,7-di(propan-2-yl)-1,3-diazatricyclo[3.3.1.1 ^{3,7}]decan-6-one	C₂₂H₃₂N₂O₃	372.5
76.	1549778	Geranylacetone	C₁₃H₂₂O	194.31
77.	1742210	Caryophyllene oxide	C₁₅H₂₄O	220.35
78.	2724856	Acetophenone	C₈H₈O	128.199
79.	3084066	Ladanein	C₁₇H₁₄O₆	314.29
80.	5280343	Quercetin	C₁₅H₁₀O₇	302.23
81.	5280794	Stigmasterol	C₂₉H₄₈O	412.7
82.	5280934	Linolenic acid	C₁₈H₃₀O₂	278.4
83.	5281167	Cis-3-hexen-1-ol	C₆H₁₂O	100.16
84.	5281515	Beta-caryophyllene	C₁₅H₂₄	204.35
85.	5281520	Humulene	C₁₅H₂₄	204.35
86.	5281764	Chicoric acid	C₂₂H₁₈O₁₂	474.4
87.	5281792	Rosmarinic acid	C₁₈H₁₆O₈	360.3
88.	5283316	2-heptenal	C₇H₁₂O	112.17
89.	5283318	4-heptenal	C₇H₁₂O	112.17
90.	5317570	Germacrene D	C₁₅H₂₄	204.35
91.	5320945	Rhamnazin	C₁₇H₁₄O₇	330.29
92.	5322111	Cis-caryophyllene	C₁₅H₂₄	204.35
93.	5364462	Z,E-213-octadecadien-1-ol	C₁₈H₃₄O	266.5

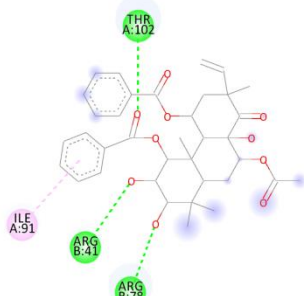
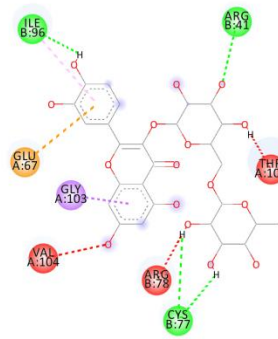
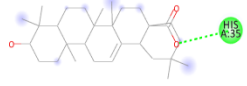
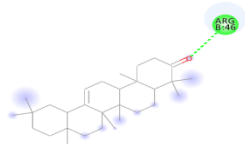
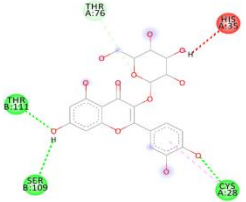
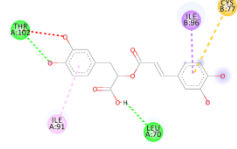
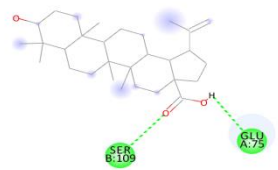
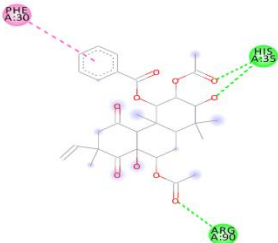
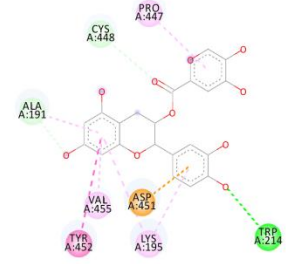
94.	5364768	E,E,Z-1,3,12-nondecatriene-5,14-diol	C₁₉H₃₄O₂	294.5
95.	5366074	Damascenone	C₁₃H₁₈O	190.28
96.	5367460	Ethyl linolenate	C₂₀H₃₄O₂	306.5
97.	5378597	Hyperin	C₂₁H₂₀O₁₂	464.4
98.	6419835	(-)-catechin gallate	C₂₂H₁₈O₁₀	442.4
99.	6428573	<u>2-[(2R,5S)-5-Ethenyl-5-Methyloxolan-2-Yl]Propan-2-Ol;</u>	C₁₀H₁₈O₂	170.25
100.	6429376	4,5-di-epi-aristolochene	C₁₅H₂₄	204.35
101.	6432254	Trans-linalool oxide	C₁₀H₁₈O₂	170.25
102.	6432312	Gamma-elemene	C₁₅H₂₄	204.35
103.	6452096	Ethyl cholate	C₂₆H₄₄O₅	436.6
104.	6918391	Beta elemene	C₁₅H₂₄	204.35
105.	9548705	Geracrene A	C₁₅H₂₄	204.35
106.	10030927	Orthosiphol M	C₃₁H₃₈O₁₀	570.6
107.	10054823	Orthosiphol X	C₃₆H₄₂O₁₀	634.7
108.	10054824	Orthosiphol K	C₃₆H₄₂O₁₀	634.7
109.	10055285	Orthosiphonone B	C₃₈H₄₂O₁₁	674.7
110.	10055454	Neoorthosiphol A	C₃₈H₄₄O₁₂	692.7
111.	10101176	Orthosiphol I	C₃₈H₄₄O₁₂	692.7
112.	10258499	Orthosiphol N	C₃₆H₄₀O₁₀	632.7
113.	10439492	Orthosiphonone A	C₃₈H₄₂O₁₁	674.7
114.	10951947	Orthosiphol V	C₃₁H₄₀O₁₀	572.6
115.	11017910	Siphonol B	C₃₈H₄₄O₁₂	692.7


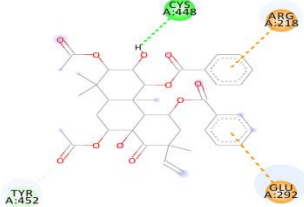
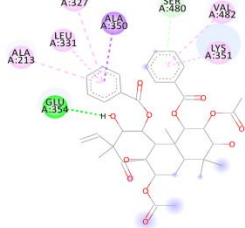
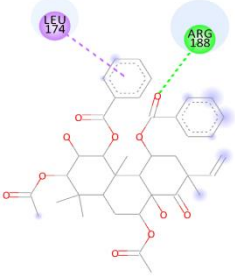
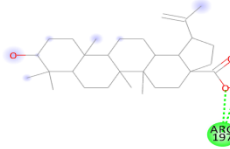
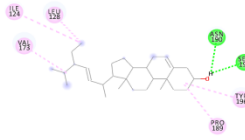
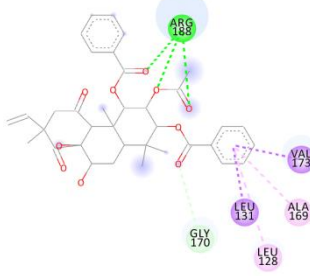
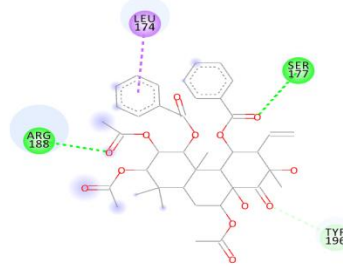
116.	11071897	Orthosiphol W	C₃₁H₄₀O₁₀	572.6
117.	11090752	Orthosiphol Z	C₂₂H₂₈O₇	404.5
118.	11115145	Siphonol C	C₃₈H₄₄O₁₂	692.7
119.	11144807	Orthosiphol Y	C₂₄H₃₂O₈	448.5
120.	11802781	Staminol B	C₃₈H₄₄O₁₂	692.7
121.	12309449	Delta-elemene	C₁₅H₂₄	204.35
122.	15385858	Orthosiphol A	C₃₈H₄₄O₁₁	676.7
123.	15385859	Orthosiphol B	C₃₈H₄₄O₁₁	676.7
124.	44246135	Isonicotinoylhydrazone of trans-2-hexanal	C₁₂H₁₅N₃O	217.27
125.	100974770	Neoorthosiphol B	C₃₈H₄₄O₁₂	692.7
126.	19725	Alpha-copaene	C₁₅H₂₄	204.35
127.	101616676	Beta-amyrone	C₂₉H₄₆O	410.7
128.	247573	Isobornyl acetate	C₁₂H₂₀O₂	196.29
129.	100965638	Orthosiphol H	C₄₅H₄₈O₁₂	780.9
130.	10952715	Siphonol A	C₄₀H₄₆O₁₃	734.8
131.	10963687	Siphonol E	C₃₉H₄₄O₁₄	736.8
132.	10628761	Staminol A	C₄₀H₄₆O₁₃	734.8
133.	5320496	Pilloin	C₁₇H₁₄O₆	314.29
134.	585744	<u>Tetracyclo[6.3.2.0(2,5).0(1,8)]Tri</u> <u>decan-9-ol, 4,4-Dimethyl-;</u> <u>CTK7J9655</u>	C₁₅H₂₄O	220.35
135.	5280805	Rutin	C₂₇H₃₀O₁₆	610.5
136.	6427080	2-octenal	C₈H₁₄O	126.2

Figure 1: Best docked compounds of *Orthosiphon stamineus* with different target proteins targeting Urolithiasis

1bt6_beta-amyrone	1bt6_orthosiphol X	1bt6_masilinic acid
		
1bt6_(-)-catechin gallate	1iqt_(-)-catechin gallate	1iqt_beta_amyrone
		
1iqt_orthosiphol X	1iqt_model1_rutin	1iqt_beta- sitosterol
		
1iqt_cianidanol	1iqt_quercetin	1kb2_(-)-catechin gallate

		
1kb2_quercetin	1kb2_A_orthosiphol A	1kb2_neoorthosiphol A
		
1poz__orthosiphol A	1poz_rutin	1poz_orthosiphol B
		
1poz_model1_masilinic acid	1poz_model1_hyperin	1poz_model1_eupatorin
		

1uuh_orthosiphol X	1uuh_rutin	1uuh_oleanolic acid
		
1uuh_beta_amyrone	1uuh_hyperin	1uuh_rosmarinic acid
		
1uuh_betulinic acid	1uuh_orthosiphol M	5fuo_A_(-)-catechin gallate
		
5fuo_A_betulinic acid	5fuo_A_orthosiphol A	5fuo_A_neoorthosiphol A

		
<p>Claudin _orthosiphol A</p>	<p>Claudin _betulinic acid:</p>	<p>Claudin _stigmasterol</p>
		
<p>Claudin _orthosiphol N</p>	<p>Claudin _staminol_A</p>	
		

Funding and Acknowledgment

This research was carried out in the Bioinformatics Laboratory, Dept. of Plant Molecular Biology and Bioinformatics, Centre for Plant Molecular Biology and Biotechnology, Tamil Nadu Agricultural University supported by the Biotechnology Information System (BTIS) program (BT/PR40235/BTIS/137/39/2022) of the Department of Biotechnology (DBT), Government of India, New Delhi.

Ethics statement

No specific permits were required for the described field studies because no human or animal subjects were involved in this research.

Consent for publication

All the authors agreed to publish the content.

Competing interests

There were no conflicts of interest in the publication of this content

Author contributions

Designed the project – Bharathi N, Performed the experiments – Bharathi.N & Caroline Nirmala.R , Drafted the manuscript – Bharathi.N & Caroline Nirmala.R. Both the authors discussed the result and reviewed the manuscript.

References

- Alelign, T., & Petros, B. (2018). Kidney stone disease: an update on current concepts. *Advances in urology*, 2018. DOI:10.1155/2018/3068365
- Asselman, M., Verhulst, A., de Broe, M. E., & Verkoelen, C. F. (2003). Calcium oxalate crystal adherence to hyaluronan-, osteopontin-, and CD44-expressing injured/regenerating tubular epithelial cells in rat kidneys. *Journal of the American Society of Nephrology*, 14(12), 3155-3166. DOI: 10.1097/01.ASN.0000099380.18995.F7
- Binkowski TA, Naghibzadeh S, Liang J. CAST p: Computed atlas of surface topography of proteins. *Nucleic Acids Res*, 2003; 31: 3352-3355. doi: 10.1093/nar/gkg512.
- Dallakyan, S., & Olson, A. J. (2015). Small-molecule library screening by docking with PyRx. *Chemical biology: methods and protocols*, 243-250. DOI: 10.1007/978-1-4939-2269-7_19
- Hsu, C. L., Hong, B. H., Yu, Y. S., & Yen, G. C. (2010). Antioxidant and anti-inflammatory effects of *Orthosiphon aristatus* and its bioactive compounds. *Journal of Agricultural and*

Food Chemistry, 58(4), 2150-2156. DOI : 10.1021/jf903557c

Kumar, V., Farrell, G., Deganello, S., & Lieske, J. C. (2003). Annexin II is present on renal epithelial cells and binds calcium oxalate monohydrate crystals. *Journal of the American Society of Nephrology*, 14(2), 289-297. DOI : 10.1097/01.ASN.0000046030.24938.0A

Kumar, M., Patel, M., Chauhan, R., Tank, C., Solanki, S., & Gami, R. (2021). Genetic analysis in ashwagandha [*Withania somnifera* (L.) Dunal. *Electronic Journal of Plant Breeding*. 12(3), 804-811..DOI: 10.37992/2021.1203.112

Letavernier, E., & Daudon, M. (2018). Vitamin D, hypercalciuria and kidney stones. *Nutrients*, 10(3), 366. DOI:10.3390/nu10030366

Ebrahimpour, A., Perez, L., & Nancollas, G. H. (1991). Induced crystal growth of calcium oxalate monohydrate at hydroxyapatite surfaces. The influence of human serum albumin, citrate, and magnesium. *Langmuir*, 7(3), 577-583. DOI : doi.org/10.1021/la00051a028

López, M., & Hoppe, B. (2010). History, epidemiology and regional diversities of urolithiasis. *Pediatric nephrology*, 25, 49-59. DOI: 10.1007/s00467-008-0960-5

Sorokina, E. A., Wesson, J. A., & Kleinman, J. G. (2004). An acidic peptide sequence of nucleolin-related protein can mediate the attachment of calcium oxalate to renal tubule cells. *JOURNAL-AMERICAN SOCIETY OF NEPHROLOGY*, 15(8), 2057-2065. DOI : 10.1097/01.ASN.0000133024.83256.C8

Tian, W., Chen, C., Lei, X., Zhao, J., & Liang, J. (2018). CASTp 3.0: computed atlas of surface topography of proteins. *Nucleic acids research*, 46(W1), W363-W367. DOI: doi.org/10.1093/nar/gky473